Millmoor Rig Wind Farm

Environmental Impact Assessment Report

(Volume 3)

Technical Appendix 6.11

Report on Light Propagation from the Aviation Warning Lights

Professor Philip Best, FRSE
School of Physics and Astronomy
University of Edinburgh

23/12/2024

Report prepared on behalf of Edinburgh Innovations Ltd, a wholly-owned subsidiary company of the University of Edinburgh

1. Introduction

1.1 The Millmoor Rig Wind Farm is a proposed development of 13 turbines with tip heights of up to 230 metres (m).

1.2 The Air Navigation Order Article 222 requires turbines exceeding a tip height of 150m to display aviation lighting to indicate their presence. Further guidance is provided in the Civil Aviation Authority (CAA) Policy Statement of 1 June 2017 entitled 'Lighting of onshore wind turbine generators in the United Kingdom with a maximum blade tip height at or in excess of 150m above ground level'. Appropriate visible lighting consists of a 2000 candela red light at the top of the turbine hub, and 32 candela red lighting at an intermediate height.

1.3 Dispensations for reduced lighting schemes can be agreed with the CAA according to the guidance provided in CAP-764. This generally involves the lighting of cardinal turbines in order to define the perimeter of the wind farm. For the proposed Millmoor Rig Wind Farm, on 20th May 2024 the CAA agreed to a reduced lighting scheme whereby only 5 cardinal turbines (turbine numbers 1, 3, 8, 9, 12; see Appendix D) require to be lit with visible lighting and the requirement for mid-tower lighting has been waived.

1.4 Should atmospheric conditions mean that visibility from the turbines is greater than 5 km, the CAA permits aviation lighting to operate in a lower intensity mode, in which the visible turbine lighting would operate at 200 candela instead of 2000 candela. Visibility sensors will be installed on the five cardinal turbines in order to measure the prevailing atmospheric conditions and visibility range.

1.5 The lighting regulations in the International Civil Aviation Organization (ICAO) Annex 14 to the Convention on International Civil Aviation relate to the luminous intensity emitted in the horizontal plane. At angles below the horizontal plane, the luminous intensity of the aviation lighting (2000 or 200 candela) is permitted to be strongly suppressed, resulting in significantly lower candela levels.

1.6 The Millmoor Rig Wind Farm is considering the use of an aircraft detection lighting scheme (ADSL), whereby the visible aviation lighting is only switched on when an aircraft is within a specified horizontal and vertical range from the wind farm. If installed, this would mean that the visible lighting would be switched off for the majority of the time.

1.7 This report provides a scientific assessment of the propagation of light from the aviation lighting, including the potential mitigation arising from the use of a vertically-suppressing aviation light fitting, and taking into account the range of atmospheric conditions typically found in Scotland and Northern England. It further considers how the human eye perceives light.

1.8 This enables an assessment of how bright the warning lights for the aviation lighting scheme for the Millmoor Rig Wind Farm will appear to be to observers external to the wind farm. Comparison is made with other sources of light, such as the moon and stars, and man-made sources.

1.9 The main body of the report discusses these issues and summarises the main conclusions, in a non-technical manner, in order to be understandable to a broad audience. Appendices to the report provide a full scientific and technical background, as well as details of the data used.

1.10 The author, Philip Best, is Professor of Extragalactic Astrophysics and Head of School in the School of Physics and Astronomy at the University of Edinburgh. He is a Fellow of the Royal Society of Edinburgh. As an observational astronomer he is familiar with issues related to the propagation of light at night, and issues of light pollution.

1.11 Professor Best has had previous involvement in studies of the effects of aviation lighting for wind farm development in Scotland, and elsewhere in the UK, both onshore and offshore, dating back to 2018.

2. Measurement and visual perception of light

2.1 Overview

2.1.1 The apparent brightness of a light, and our perception of it, depends on many factors. These include:

- How intrinsically powerful the light is
- Whether the light is emitted equally in all directions
- The colour of the light
- The distance of the observer from the light
- The nature of the atmosphere through which the light passes
- The background lighting conditions in which the light is viewed
- The response of the human eye

2.1.2 This report will examine all of these issues to calculate the apparent brightness for observers of the aviation lighting at the proposed Millmoor Rig Wind Farm.

2.2 Terminology and propagation of light

2.2.1 This section provides a brief overview of the propagation of light, and relevant terminology. For a more detailed technical discussion, see Appendix A.

2.2.2 The regulations on aviation warning lights are expressed in terms of *candela* requirements. Candelas are a measure of the *luminous intensity* of the light. Luminous intensity measures the amount of light, at wavelengths detectable by the human eye, which is emitted in a particular direction.

2.2.3 If a light emits anisotropically (i.e. different amounts of light in different directions) then its candela rating will depend upon direction.

2.2.4 More distant light sources appear fainter, because the light emission spreads out over a larger area. The observability of light depends upon the *illuminance* of the light, which measures the luminous intensity of light that passes through a unit area of surface at that distance. Illuminance is measured in *lumens per square metre*.

2.2.5 It is the illuminance of the light that determines how bright it appears to the observer. This is the key quantity that this report will be deriving for the aviation lighting and comparing to the illuminance of other light sources.

2.2.6 For perfect transmission of light (i.e. no light absorbed or scattered by the medium through which it is passing), the illuminance decreases as the square of the distance between the light source and the observer. Thus, a light observed from a distance of 10km will have an illuminance only 1% of that of the same light observed from a distance of 1km.

2.3 Human perception of light

2.3.1 The human eye is composed of two different types of optical sensors, known as *cones* and *rods*, each of which is adapted to function under different light conditions to maximise the overall ability of the eye (see Appendix B for a more detailed technical discussion).

2.3.2 Cone cells provide the ability for humans to discern colour. Cones are adapted to work at high ambient light levels; this is known as the *photopic* regime.

2.3.3 In contrast, rods have no ability to identify colour, but do have a much higher sensitivity than cones, allowing fainter levels of light to be detected (albeit that in such light levels the eye loses the ability to distinguish colour and objects appear grey). Rods mediate vision at low ambient light levels, known as the *scotopic* regime.

2.3.4 At intermediate light levels both cones and rods play a role; this is known as *mesopic* vision. It is not as sensitive as scotopic vision, but does allow for perception of colour.

2.3.5 In the photopic regime (daytime vision) the human eye is most sensitive to green light.

2.3.6 Luminosity intensity and illuminance are both calculated in a way that weights the colour distribution of the light with the photopic (daytime) wavelength response of the human eye. Thus, in high ambient light conditions, a blue and a red light of the same luminous intensity (candela rating), seen at the same distance, will appear equally bright.

2.3.7 In the scotopic regime (night-time vision) the eye is more sensitive to bluer light and has little sensitivity to red light. Therefore, at low ambient light levels (in the mesopic or scotopic regimes), a red light will appear fainter than a blue light of the same candela rating at the same distance.

2.3.8 The threshold sensitivity of the eye depends critically on the background ambient light level. It also varies to some extent from observer to observer (e.g. due to deterioration with age).

2.3.9 Maximum sensitivity is achieved in the darkest ambient conditions, but only after the eye has become fully dark-adapted. Dark adaptation is associated with chemical changes in the eye and is largely complete after around 30 minutes of darkness. Any (even short) exposure to bright light resets the dark adaptation process.

2.3.10 Fully dark-adapted eyes in optimal observing conditions (moonless night-time sky, away from sources of light pollution) have a typical sensitivity limit of just below 10^{-8} lumens/m^2 to a point source of white light. That sensitivity limit is fractionally higher (approximately $2x10^{-8}$ lumens/m^2) for red light, limited by the lower end of the mesopic regime.

2.3.11 Infrared lighting, produced to Ministry of Defence standards, emits in the wavelength range 750 to 900nm. The eye has essentially no sensitivity at these wavelengths, and therefore the installation of infrared lights on the turbines in the proposed wind farm will have no visual impact. The infrared lighting is not considered further in this report.

3. Atmospheric attenuation of light

3.1 Atmospheric attenuation in 'clear' conditions

3.1.1 As light passes through the atmosphere, it is attenuated (decreased in brightness) by scattering and absorption processes in the atmosphere. A full technical description of this process is presented in Appendix C. Here, an outline summary is provided.

3.1.2 The attenuation process is caused both by the molecules of air in the atmosphere and by microscopic solid or liquid particles suspended in the atmosphere, known as aerosols. Aerosols can be natural, such as dust and pollen, or man-made pollutants, such as smoke or vehicle emissions. In maritime environments, sea salt is prevalent. Another common aerosol is liquid water droplets suspended in the air, as is the case for cloud or fog.

3.1.3 The total amount of attenuation depends upon amount of material through which the light passes (known as the optical depth, or opacity, of the material). For light travelling horizontally through the atmosphere, the optical depth is proportional to the distance between the light source and the observer.

3.1.4 The optical depth is also dependent upon the wavelength of the light. The exact wavelength dependence is determined by the properties of the attenuating material, but in general blue light is more strongly attenuated than red light.

3.1.5 Attenuation by air molecules occurs due to a process known as Rayleigh Scattering. This is well-quantified, and varies little with time. As outlined in Appendix C, it can be calculated with high accuracy. Rayleigh scattering has a very strong wavelength dependence, with blue light being much more highly scattered (this is the reason that the sky appears blue).

3.1.6 The attenuation by aerosols can be estimated (see Appendix C) but, unlike Rayleigh Scattering, this cannot be described by a single number. The quantity and nature of aerosols varies with location and over time (for example, due to the direction that the wind is coming from). This changes the optical depth of the aerosols, the wavelength dependence of the scattering process, and the vertical distribution of aerosols in the atmosphere.

3.1.7 Extensive ground-based measurements of the distribution of properties of aerosols exist in different UK environments, and these are complemented by satellite observations. Based upon these, predictions can be made for the range of levels of attenuation of light by aerosols (see Appendix C), as a function of distance, for typical 'clear' conditions.

3.1.8 Considering this range, the calculations in Appendix C of the atmospheric attenuation of red light show that between 55% and 80% of the light remains, when viewed horizontally from a distance of 10km, at an altitude of 390m (the average hub height altitude of the turbines with visible aviation lighting in the Millmoor Rig Wind Farm).

3.1.9 The geometric dilution of light with distance (see 2.2.6) is then scaled by this attenuation factor to determine the final observed illuminance of the light. Given the strong geometric dilution effects compared to the relatively mild atmospheric attenuation at distances below 10-15km, the choice of adopted aerosol parameters (for 'clear' conditions) does not qualitatively change the conclusions.

3.2 Visibility

3.2.1 The Air Navigation Order regulations (Article 222) and the CAA Policy Statement of 1 June 2017 ('Lighting of onshore wind turbine generators in the United Kingdom with a maximum blade tip height at or in excess of 150m above ground level') require relevant turbines to be lit with a 2000 candela light, but this may be reduced to 200 candela if the visibility is better than 5km.

3.2.2 Visibility has a standard definition (from the World Meteorological Organisation) as the distance at which the intrinsic brightness of a light is reduced to 5% of its initial value due to light attenuation. It is thus directly related to optical depth.

3.2.3 In poor visibility conditions, the opacity is generally associated with larger aerosols such as liquid water droplets (cloud or fog).

3.2.4 The illuminance of a light can be accurately calculated as a function of distance, for the aerosol density which gives the threshold visibility value of 5km. This represents the worst-case scenario for 2000 candela lighting considered in this report. Typically, in better conditions the luminous intensity of the lighting can be reduced, while in poorer conditions atmospheric attenuation effects will be increased.

3.2.5 The fraction of time for which the visibility is below 5km would ideally be determined using on-site measurements. However, estimates can be made by considering publicly-available datasets from other locations within Scotland and Northern England.

3.2.6 An extensive dataset from the Leuchars air base in Fife (115km from the Millmoor Rig Wing Farm) provides data on the historic visibility dating back several decades (Singh et al. 2017). The 5km visibility threshold for requirement of the 2000 candela lights is only met at Leuchars between 3% and 4% of the time in the last 20 years.

3.2.7 Met Office data from Carlisle airport (48km from the Millmoor Rig Wind Farm) indicates a similar fraction of between 5 and 6% of the time when visibility is below 5km. Data from airports around southern Scotland (some close to large population centres and subject to higher man-made aerosol pollutants) also provide typical values of between 4% and 7% of the time, in line with the Carlisle airport and Leuchars results. Statistics from Newcastle airport (65km from the wind farm), however, indicate a higher prevalence of poor visibility, around 11% of the time.

3.2.8 Many of these datasets are obtained close to sea level. Although aerosol density decreases with increasing altitude, higher altitude sites like that of the proposed Millmoor Rig Wind Farm may be more susceptible to periods of mist or cloud. For this reason, a reasonable estimate is that the Millmoor Rig Wind Farm may be affected by poor visibility (and hence require the use of 2000 candela lighting) for up to 10% of the time.

4. Illuminance of aviation lighting

4.1 Illuminance of individual turbine lights

4.1.1 Following the detailed calculations of Appendix C, the illuminance of individual turbine lights, as a function of distance, is shown in Figure 1. These are calculated for 'clear' atmospheric conditions for a luminous intensity of 200 candela. Results are shown for average assumptions of the aerosol attenuation.

4.1.2 Also shown on Figure 1 are the results for 2000 candela lights as observed at the threshold visibility limit of 5km (i.e. the worst-case scenario for these lights). In the poor visibility conditions when they are required, these 2000 candela lights have lower illuminance than the 200 candela lights seen in typical clear conditions, for all distances beyond 5km.

4.1.3 For comparison with these calculations, Figure 1 also shows the illuminance of the brightest star in the northern sky, and of typical bright stars such as those in the constellation of Orion. The latter provide a good approximation of the limiting illuminance that can be observed from street-lit locations. Also shown is the approximate visible limit under optimal conditions: fully dark-adapted eyes away from any light pollution. Table 1 provides numerical values for these illuminances, and also the illuminance of car brake lights at different distances, which provide a natural comparison.

4.1.4 Figure 1 and Table 1 make clear that from a distance of 5km, both the 200 candela light in clear conditions and the 2000 candela light in poor visibility have illuminances below that of the brightest star, and comparable to car brake lights seen from distances of a few km. At larger distances from the turbines, the 2000 candela light (in poor visibility) quickly becomes unobservable. The illuminance of the 200 candela light is comparable to that of typical bright stars at distances of 10-15km, reaching the observable threshold from street-lit areas by a distance of about 15km.

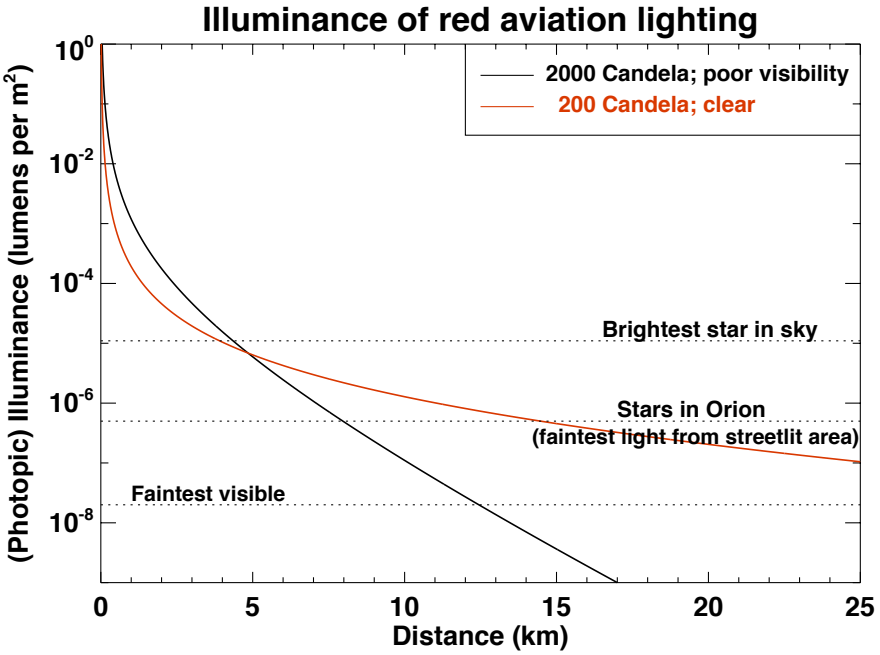

Figure 1: The illuminance of a single red light (wavelength 633nm) as a function of distance, viewed horizontally at an altitude of 390m. The results are shown for a light with a luminous intensity of 200 cd for typical 'clear' atmospheric conditions. Also shown are the results for 2000 cd lights, at the threshold visibility (visibility=5km) that these are required. For comparison, the illuminance provided by the brightest star in the northern sky is shown, along with those of typical bright stars such as those in the constellation of Orion. The latter also represent the approximate visual limit of the eye from street-lit areas (see Appendix B). Also indicated is the approximate visible limit to red light under perfect conditions (away from street lighting and other light pollution; new moon; dark-adapted eyes).

Comparison object	Approx. Illuminance (Lumens per m^2)
Car brake lights at 1km distance	100×10^{-6}
Brightest star in the sky	13×10^{-6}
Car brake lights at 10km distance	1×10^{-6}
Typical bright stars (e.g. in Orion)	0.5×10^{-6}
Faintest light visible from street-lit area	0.4×10^{-6}
Visible limit for fully dark-adapted eyes	0.02×10^{-6}

Table 1: Illuminances of typical comparison objects.

4.1.5 It is important to note that Figure 1 assumes that the aviation lighting is seen horizontally. The regulations in the International Civil Aviation Organization Annex 14 to the Convention on International Civil Aviation relate to the luminous intensity emitted in the horizontal plane. At angles below the horizontal plane, the luminous intensity of modern aviation lighting (2000 or 200 candela) can be strongly suppressed, resulting in significantly lower illuminance. This is shown in Figure 2 which presents technical data from an aviation light currently on the market.

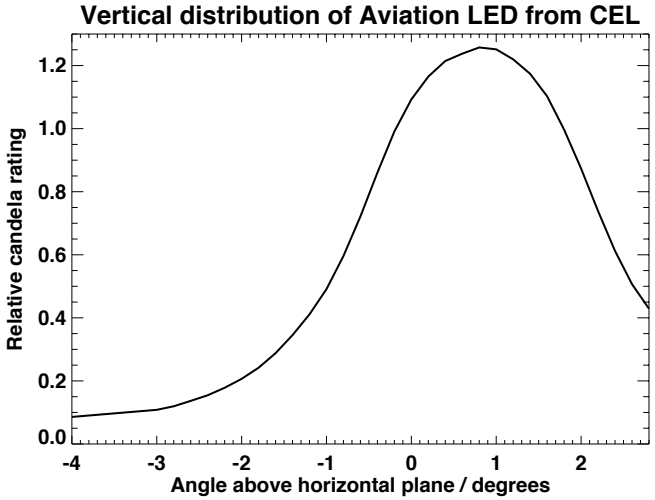

Figure 2: The attenuation of the illuminance of aviation lighting away from the horizontal plane. The figure shows technical data for an aviation Light-Emitting Diode (LED) currently on the market, from the supplier Contarnax Europe Ltd (CEL). At an angle of 3 degrees below the horizontal plane, the brightness of the lights is suppressed by a factor of 10. Note that other lights available in the market may give rise to different levels of suppression at both positive and negative angles of elevation, depending on their design characteristics, but due to ICAO regulations are not likely to be substantially different.

4.1.6 This vertical suppression will be relevant both for observers close to the turbines (who will typically be viewing them from below) and for nearby population centres which are located at lower altitude than the Millmoor Rig Wind Farm.

4.1.7 For the Millmoor Rig Wind Farm, the locations of the proposed turbines, along with details of which turbines will carry visible lighting in the CAA-approved lighting scheme, are provided in Appendix D. Appendix D also provides the locations and details of the 21 representative viewpoints considered in the Landscape and Visual Impact Assessment (LVIA), and from which this report will explicitly consider the brightness of the aviation lighting. Other associated LVIA documents present visual representation from the LVIA viewpoints, and Zone of Theoretical Visibility (ZTV) diagrams for the turbines, including a lighting intensity ZTV.

4.1.8 Table 2 provides the calculated illuminance of the brightest turbine light for the approved lighting scheme of the Millmoor Rig Wind Farm, as seen from each of 21 representative LVIA viewpoints. Values are calculated taking into account the propagation of light (Figure 1) and are provided both with and without consideration of the suppression of light relative to the horizontal plane (Figure 2). Values are given for both average 'clear' conditions (with a 200cd light) and for the limit of 'poor visibility' conditions (with a 2000cd light). Table 1 provides every-day visual comparators to the calculated illuminances.

Viewpoint		Brightest Turbine			Illuminance with no vertical suppression (lumens per square metre)		Illuminance assuming suppressing aviation light fitting (lumens per square metre)	
Nº	**Name**	**Nº**	**Distance (km)**	**Vertical suppression factor**	**200 cd average conditions**	**2000 cd poor visibility**	**200 cd average conditions**	**2000 cd poor visibility**
1	A6088 Chesters	8	3.37	0.13	15.1×10^{-6}	30.5×10^{-6}	2.01×10^{-6}	4.04×10^{-6}
2	A6088 Southdean	3	2.41	0.10	30.9×10^{-6}	98.5×10^{-6}	3.04×10^{-6}	9.68×10^{-6}
3	Fort NE Southdean	3	2.67	0.35	24.9×10^{-6}	69.8×10^{-6}	8.77×10^{-6}	24.6×10^{-6}
4	A6088 W. Chesters	8	3.47	0.14	14.2×10^{-6}	27.2×10^{-6}	2.02×10^{-6}	3.87×10^{-6}
5	Bonchester Hill	8	5.17	0.79	5.94×10^{-6}	5.10×10^{-6}	4.71×10^{-6}	4.04×10^{-6}
6	B6357 Vantage Pt	12	2.88	0.50	21.2×10^{-6}	53.8×10^{-6}	10.5×10^{-6}	26.7×10^{-6}
7	Path Knox Knowe	1	3.38	1.21	15.1×10^{-6}	30.2×10^{-6}	18.2×10^{-6}	36.6×10^{-6}
8	A6088 NW Carter	3	4.12	0.98	9.79×10^{-6}	13.8×10^{-6}	9.63×10^{-6}	13.6×10^{-6}
9	Carter Bar	3	6.30	1.24	3.80×10^{-6}	1.90×10^{-6}	4.72×10^{-6}	2.37×10^{-6}
10	Pike Fell	9	7.10	0.98	2.89×10^{-6}	0.99×10^{-6}	2.82×10^{-6}	0.97×10^{-6}
11	Chesters Brae	8	3.92	0.33	10.9×10^{-6}	16.9×10^{-6}	3.63×10^{-6}	5.61×10^{-6}
12	Rubers Law	8	9.17	1.18	1.58×10^{-6}	0.20×10^{-6}	1.86×10^{-6}	0.24×10^{-6}
13	Bonchester Bridge	9	7.53	0.38	2.52×10^{-6}	0.70×10^{-6}	0.95×10^{-6}	0.27×10^{-6}
14	Wolfelee Hill	9	1.97	0.45	47.2×10^{-6}	184.9×10^{-6}	21.0×10^{-6}	82.5×10^{-6}
15	Pen.Way, Black Halls	3	15.83	1.20	0.39×10^{-6}	$<0.01 \times 10^{-6}$	0.47×10^{-6}	$<0.01 \times 10^{-6}$
16	Five Stanes	3	15.53	1.00	0.41×10^{-6}	$<0.01 \times 10^{-6}$	0.42×10^{-6}	$<0.01 \times 10^{-6}$
17	A7 Hawick	9	13.86	0.47	0.56×10^{-6}	$<0.01 \times 10^{-6}$	0.27×10^{-6}	$<0.01 \times 10^{-6}$
18	Borders Abbey Wy	8	11.04	1.02	1.00×10^{-6}	0.05×10^{-6}	1.02×10^{-6}	0.05×10^{-6}
19	Wheel Causeway	12	3.46	1.16	14.3×10^{-6}	27.8×10^{-6}	16.6×10^{-6}	32.2×10^{-6}
20	A68 N Carter Bar	9	8.62	0.47	1.83×10^{-6}	0.30×10^{-6}	0.86×10^{-6}	0.14×10^{-6}
21	Rowan Rd Jedburgh	-	-	-	-	-	-	-

Table 2: Calculated illuminances of the brightest turbine aviation light visible from the designated viewpoints. Full viewpoint details can be found in Appendix D. Table 1 provides every-day comparisons to the illuminances quoted. Calculations are provided for both a 200 cd light under average 'clear' atmospheric conditions and a 2000 cd light at the limit of the poor visibility conditions (visibility=5km) when such a light is required. Calculations are provided both with no vertical suppression considered, and also taking into account the vertical suppression of light away from the horizontal plane, assuming the LED specifications of a commercially-available aviation light from CEL (see Figure 2). Note that none of the turbine lights is visible from viewpoint 21.

4.1.9 The closest LVIA representative viewing point for the proposed Millmoor Rig Wind Farm is on Wolfelee Hill (viewpoint 14) at a distance of just under 2km from the nearest lit turbine. Under typical 'clear' conditions, receptors at this location will observe the aviation lights to be between 3 and 4 times brighter than the brightest star in the night sky if no vertical suppression is considered, or just under twice as bright if suppression aviation lights are used. The turbine lighting would appear to be of equivalent brightness to car brake lights at a distance of 1.5 km (without suppression) or 2.2 km (with suppression). From this location the lighting will thus be clearly visible.

4.1.10 From the closest residential viewpoints, at Chesters (viewpoint 1) and Southdean (viewpoint 2), the aviation lights would be comparable to, or slightly brighter than, the brightest star in the sky under typical clear conditions, ignoring vertical suppression. However, these locations are at lower altitude than the wind farm, and so suppression aviation lighting would reduce the apparent brightness by a factor of 8 to 10, resulting in apparent brightnesses of just a few times brighter than typical bright stars such as those in Orion, equivalent to car brake lights at distances of 7 or 8 km. Under these circumstances the lights would therefore be visible, but not prominent.

4.1.11 From more distant larger population centres, such as Hawick (viewpoint 17) at a distance of around 14 km, the larger distance to these viewing points leads to fainter expected illuminances, which are comparable to those of bright stars like Orion if viewed without suppression. Receptors at this locations will observe the aviation lights from angles of around 1 degree below the horizontal plane, leading to potential suppression of the brightness by a factor of about 2. Including such suppression, the expected illuminances would be around, or just below, the level of the faintest lights visible from street-lit areas: under typical atmospheric conditions such aviation lighting would be visible to dark-adapted eyes at this viewpoint but would be faint.

4.1.12 In periods of poor visibility, when the 2000cd lights need to be used, Table 2 shows that for the more distant viewing points (beyond ~5km) these will appear fainter than the 200cd lights would be in normal conditions; indeed, from the most distant viewpoints the 2000cd lights would not be visible in poor conditions, even to fully dark adapted eyes. At the closest residential viewing points, Chesters and Southdean, the 2000cd lights in poor visibility conditions would be 2-3 times brighter than the 200cd lights in normal conditions, but would still be fainter than the brightest star in the sky if aviation lighting with vertical suppression is installed.

4.1.13 It is worth noting that there may be exceptional circumstances (e.g. if part of the wind farm is in cloud and another part is not in cloud) where 2000cd lighting is required but the visibility towards a particular turbine is not poor. In such a case, the illuminance of the lighting might be 10 times brighter than that calculated for the 200cd light in average conditions. However, such circumstances are expected to be rare.

4.1.14 Finally, it should be highlighted that if an aircraft detection lighting scheme (ADSL) in installed, then the above calculations correspond only to the periods of time when the aviation lighting is switched on, due to the presence of an aircraft within a specified horizontal and vertical range from the wind farm. With ADSL in operation, the visible lighting would be switched off for the majority of the time.

4.2 Additional considerations

4.2.1 The total illuminance from all turbine lights within the wind farm (calculated in Appendix C7) is comparable to, or below that, produced by starlight in a moonless sky, beyond an average distance of about 3km from the turbines. Thus, other than the individual points of light visible from individual turbines, outside of the wind farm there will be no significant change to the ambient light levels, and hence on the nature of 'dark skies'.

4.2.2 A common concern is that, during the hours of darkness, when turbine blades pass in front of the aviation lights they will appear to flicker. Although this is true, it should be noted that lights in the night sky naturally flicker (stars 'twinkle') due to atmospheric refraction effects. As discussed above, at the more distant viewpoints considered, the illuminances of the turbine lights are comparable to those of stars: any such flickering will therefore be consistent with other similar brightness lights in the night sky. From the closest viewpoints, especially if the aviation lighting does not include vertical suppression, the brighter illuminance combined with the red colour of the lighting will allow any flickering to be more noticeable. However, this will still not be significantly more than that of stars, and so this is unlikely to be a major cause of concern.

5. Summary

5.1 This report has considered the observability of the aviation lighting for proposed Millmoor Rig Wind Farm. The report takes into account the brightness of the lights, geometric dilution of light, atmospheric attenuation, and the response of the human eye.

5.2 At distances of 5-15 km, 200 candela lights, which will be lit on the turbines under typical atmospheric conditions, will have an apparent brightness comparable to that of bright stars in the night sky, or to car brake lights at a distance of 3-10km. They will thus be visible to observers with a degree of dark adaptation, but will not be prominent. The lights will remain visible to fully dark-adapted eyes out to distances of 30-40km, but their prominence falls further still.

5.3 When the visibility is sufficiently poor as to require 2000 candela lighting, then the visual impact of these beyond 5km distance will be less than that of the 200 candela lights.

5.4 The reduction of light intensity below the horizontal plane for some modern aviation lighting means that, in reality, from most nearby locations any impact could be even further reduced, by up to a factor of 10, if suppression aviation light fittings are installed.

5.5 The impact of the aviation lighting is illustrated through consideration of the illuminance of the brightest turbine light from the designated viewpoints. From the closest residential viewpoints (at distances of 2-4 km), the illuminance of the aviation lighting under typical night-time conditions is calculated to be a few times fainter than the brightest star in the sky, if vertical suppression of the lighting is taken into account. This conclusion also holds during the periods when the visibility is poor and the 2000 candela lighting is required. From larger, most distant population centres such as Hawick, the combination of the distance to the wind farm and the vertical suppression of the lighting leads to the lighting being faint: it will appear fainter than typical bright stars in the sky, and only be visible to observers with partially dark-adapted eyes.

Appendix A: Terminology and propagation of light

A.1 The measure of how intrinsically powerful a light source is (its *power*, or *radiant flux*) is the amount of energy that it emits each second. This is measured in *Watts.* A familiar example will be a standard domestic light bulb (e.g. a 60 Watt light bulb).

A.2 This energy emitted by a light can be spread across a wide range of wavelengths (colours); some of these are not detectable by the human eye (see Appendix B for a technical discussion of the eye's sensitivity). The amount of energy per second emitted, weighted by the (daytime) sensitivity of the human eye at different wavelengths, is known as *luminous flux* and is measured in *lumens.*

A.3 Another commonly used measure of the intrinsic brightness of a light source is the *luminous intensity.* This is defined as the luminous flux emitted per unit solid angle in a given direction. Solid angle is a measure of angular area, measured in *steradians*. The solid angle of the full surface of a sphere is 4π steradians (thus 1 steradian is approximately 3283 square degrees).

A.4 For an isotropic light source (i.e. one that emits light equally in all directions) the luminous intensity is simply the luminous flux scaled down by the factor of 4π. If a light emits anisotropically (i.e. different amounts of light in different directions) then the luminous intensity will vary with direction.

A.5 Luminous intensity is measured in *candelas.* Aviation warning light regulations are expressed in terms of candela requirements.

A.6 More distant light sources appear fainter, because the light emission spreads out over a larger area. The observability of light depends upon the *illuminance* of the light, which measures the luminous intensity of light that passes through a unit area of surface at that distance. Illuminance is measured in *lumens per square metre* (also known as *lux*). It is the illuminance of the light that determines how bright it appears to the observer.

A.7 For perfect transmission of light (i.e. no light absorbed or scattered by the medium through which it is passing), the illuminance (I) is related to the luminous intensity (L) by:

$$I = \frac{L}{D^2}$$

where D is the distance between the light source and the observer in metres.

A.8 Figure A1 shows examples of illuminance as a function of distance for lights of 200 and 2000 candela luminous intensities, in the absence of any attenuation effects (see Appendix C).

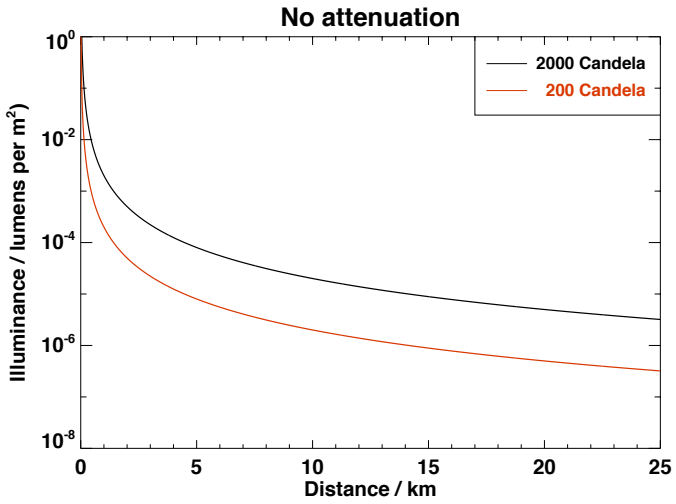

Figure A1: The illuminance of 2000 candela and 200 candela luminous intensity lights as a function of distance, in the absence of any atmospheric attenuation (i.e. considering geometric effects only).

Appendix B: The response of the human eye to light

B.1 Optical sensors in the eye

B1.1 The human eye is composed of two different types of optical sensors, known as *cones* and *rods*.

B1.2 Cones are concentrated in the central portion of the retina, and provide the sharpest vision. Cones come in three types adapted to detect different wavelengths of light (approximately, blue, green and red light respectively). The combination of light detected by these three types of cone cells provides the ability for humans to discern colour. Cones are adapted to work at high ambient light levels, (above a few candela/m^2), which is known as the *photopic* regime.

B1.3 Rods are more distributed around the retina. Rods have a much higher sensitivity than cones, allowing fainter levels of light to be detected. Rods mediate vision in the *scotopic* regime, corresponding to ambient light levels below about 0.003 candela/m^2. Rods have no colour response, and so in these low light levels the eye loses the ability to distinguish colour and objects appear grey.

B1.4 Because rods are spread across the eye, and largely absent from the (cone-dominated) central region, this gives rise to the well-known effect that in low ambient light levels, faint light sources appear clearer in peripheral vision than when looked at directly.

B1.5 The eye's sensitivity function has been formalised by the International Commission on Illumination (CIE). In the photopic regime, the widely used standard is the CIE 1978 V(λ) function, based on data by Judd (1951) and Vos (1979): this is shown in Figure B1 and has maximum sensitivity at a wavelength of 555nm (green).

B1.6 Figure B1 also shows the CIE 1951 V'(λ) sensitivity function of the eye in the scotopic regime, which is based on measurements by Wald (1945) and Crawford (1949). Here it can be seen that the peak sensitivity is at significantly shorter wavelength than the photopic curve (507nm), and that the sensitivity at longer (redder) wavelengths is dramatically lower in the scotopic regime. In particular, at the wavelength of standard red aviation LEDs (633nm) it is nearly a factor 100 lower.

B1.7 At intermediate light levels both cones and rods are activated; this is known as *mesopic* vision. It is not as sensitive as scotopic vision, but does allow perception of colour. The eye sensitivity in mesopic vision depends upon the relative stimulation of the cones and rods. As indicated on Figure B1 there is a gradual change of the sensitivity function as we move down the mesopic regime. At all points, the sensitivity to red LEDs will be dominated by whatever component of photopic vision remains.

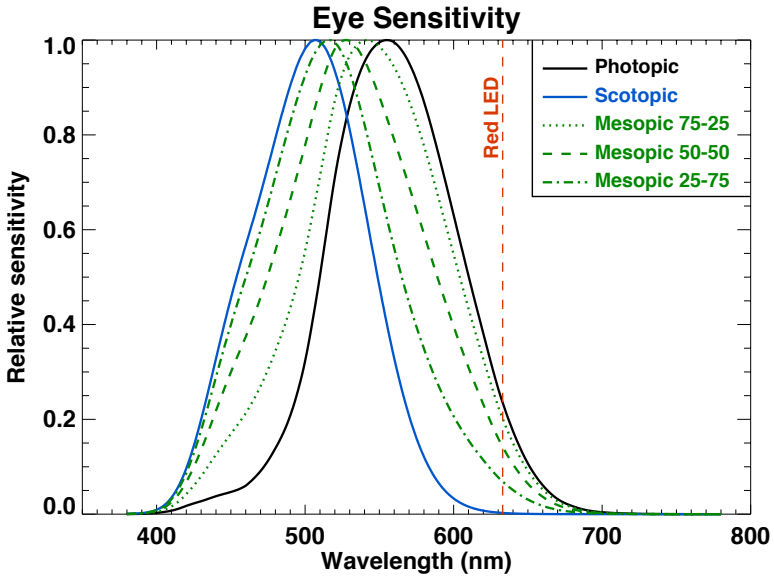

Figure B1: The relative sensitivity of the eye as a function of wavelength, in the photopic regime (black line; vision mediated by cones, at high light levels) and the scotopic regime (blue line; vision mediated by rods, at low light levels). The data are the accepted CIE 1978 and CIE 1951 standard values (see text for details). At low light levels the eye sensitivity function shifts towards bluer wavelengths, with significantly lower relative sensitivity to red light. Also shown in green lines are intermediate stages of mesopic vision, where both cones and rods are activated (dotted, dashed and dot-dashed lines show respectively a 75%-25% split, a 50%-50% split, and a 25%-75% split between photopic and scotopic vision).

B1.8 The conversion of radiant flux to luminous flux is normally derived by weighting the radiant flux by the photopic sensitivity function. Thus, in the photopic regime, a light of given luminous intensity viewed from a given distance will appear to deliver the same illuminance irrespective of its colour: in other words, from a given distance, a blue light and a red light emitting the same candela of light would appear equally bright.

B1.9 However, if the light level is sufficiently low that the eye enters the mesopic or scotopic regime, then the shift of the eye's sensitivity function towards shorter wavelengths would result in a redder light appearing fainter than a bluer one.

B.2 Eye detection thresholds

B2.1 Studies of the detection threshold of the eye (that is, the faintest detectable illuminance for a single fixed light) have a long history; for example, it is of wide interest in astronomy to understand the faintest star visible under different light pollution conditions, and that analysis is directly relevant here.

B2.2 The most authoritative and extensive data samples were taken by Blackwell (1946), supplemented by the work of Knoll et al. (1946), who studied the detectability of point sources of light by the eye in different ambient lighting

conditions. Specifically, they considered background illumination levels (B), and tested the ability of observers to detect point source lights of incremental illuminance (ΔI) above this background. The primary results are shown in Figure B2 and have largely been supported by later studies.

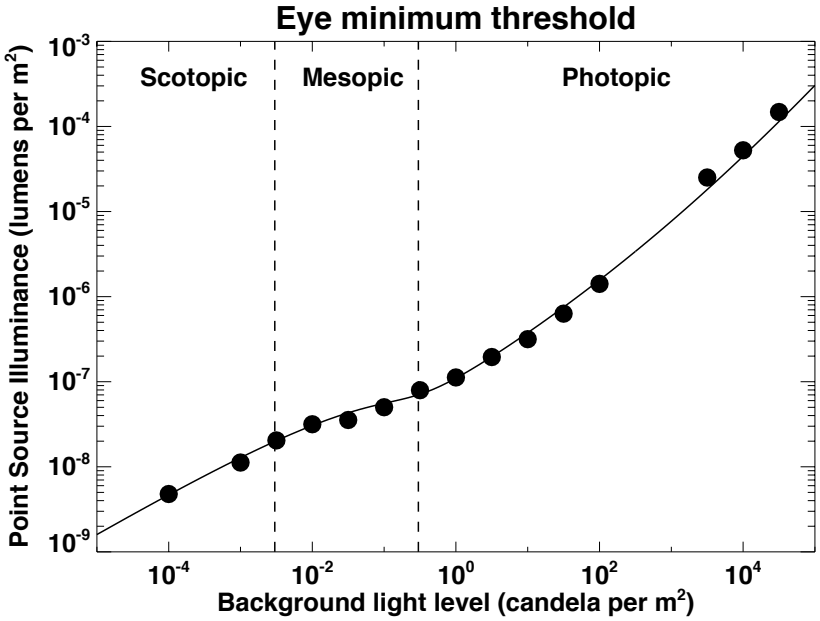

Figure B2: The minimum point source illuminance, which is detectable by the eye, as a function of the background ambient light level. Plotted data points are from Knoll et al. (1946), and the fitting function comes from Crumey (2014).

B2.3 There have been many attempts to provide functional fits to these data. The best of these consider separate functional forms in the photopic and scotopic regimes, as it is clear from Figure B2 that the detectability of light is non-linear due to the changes between the different vision regimes. The fit shown in Figure B2 comes from Crumey (2014), and is the one adopted for the current analysis.

B2.4 These results are based on a white light source (i.e. one that emits across a very wide range of wavelengths); the colour temperature of the white light (that is, the exact distribution of radiant flux across wavelength) will have an effect on the derived threshold in the mesopic and scotopic regime, but this will typically lead to variations of well below a factor of 2.

B2.5 Note that these data are based on the average results from young adults (less than 30 years old) in fully dark-adapted conditions. Those who have not taken the time to dark-adapt their eye in low lighting conditions, will have significantly higher detectable limits.

B2.6 Dark adaptation is a relatively slow process associated with chemical changes in the eye. Dark adaptation of the cones to lower light levels takes between 5 and 10 minutes. Rods are nearly fully activated after about 30 minutes, although the sensitivity of rods to low light levels continues to improve marginally even after hours of darkness. Even a short exposure to bright light resets this process. An observer in a partially lit environment (e.g. street lighting) never becomes fully dark adapted.

B2.7 Older people typically take longer to dark-adapt, and generally have significantly higher detectable limits. Blackwell & Blackwell (1971) estimate a factor approximately 3 higher threshold on average at age 65.

B.3 Ambient background lighting levels and limiting sensitivities

B3.1 Figure B2 indicates that the detectable limit of light depends strongly on the background ambient light level. This can vary considerably, depending on location and on moon phase.

B3.2 In a street-lit area, the ambient light level is about 10 candela/m^2. From Figure B2, this gives a faintest detectable illuminance of a (white) point-source light of around $5x10^{-7}$ lumens/m^2. To put this value into context, this is about the same apparent brightness as typical bright stars in the night sky, such as the main stars in the constellation of Orion, or of a car brake light seen from a distance of about 10 km.

B3.3 The darkest night-time conditions are found for a new moon, and away from any source of light pollution. For this, the ambient light level due to starlight from all of the stars in the sky is around $2x10^{-4}$ candela/m^2. The corresponding faintest detectable illuminance is around $6x10^{-9}$ lumens/m^2.

B3.4 Falchi et al. (2016) studied the sky brightness as a function of location in Europe; their data indicate that the background light level away from towns in the region of the Millmoor Rig Wind Farm is around twice the level of the dark sky background. Cinzano et al. (2001) found a similar result for the increased sky brightness due to airglow. Their limiting brightness in that region of Scotland corresponds to an illuminance of a little above 10^{-8} lumens/m^2. This value provides a more realistic estimate of the limit of the detectability of a white light source in optimal new moon conditions.

B3.5 For red LED aviation lighting at 633nm, the sensitivity of rods is a factor approximately 100 below that of the cones (see Figure B1). Thus, if the ambient light level were to be sufficiently low as to be fully in the scotopic regime, then faint red lights become largely undetectable. A realistic detectable limit for faint red lights is at the bottom of the mesopic regime, at an illuminance of around $2x10^{-8}$ lumens/m^2.

Appendix C: Attenuation of light

C.1 Overview

C1.1 Light is attenuated by scattering and absorption processes as it travels through the atmosphere. The attenuation is described by the *optical depth* of the attenuating medium, τ, such that the un-attenuated fraction of light (f) is given by:

$$f = \exp(-\tau)$$

where exp is the exponential function.

C1.2 The optical depth depends upon the amount of attenuating material that the light passes through. This can be written as

$$\tau = \sigma \int n \, dl$$

where σ is the cross-section of the absorber or scatterer, *n* is the number density of the scatters, and the integral over *dl* is an integral along the path from the source to the observer.

C1.3 In the case of light travelling horizontally through the atmosphere near the surface of the Earth, the number density of scatterers can be estimated to be constant along the line of sight, and so the optical depth scales proportionally to the distance (D). This can be written as

$$\tau = \tau_0 \left(\frac{D}{1\text{km}}\right)$$

where τ_0 is the optical depth for a characteristic distance of 1km.

C1.4 The value of τ_0 depends on the properties of the atmosphere, and also depends on the wavelength of the light that is being observed.

C1.5 The value of τ_0 is also dependent upon altitude, since the density of scatterers depends upon altitude.

C1.6 If the observer and the light source are at different altitudes then a full integral of the equation in C1.2 is formally required, rather than the simplification in C1.3. However, differences in calculated illuminance are small. Furthermore, where different altitudes are involved, the suppression of the beam of the aviation light away from the horizontal plane has a far more significant effect on the resultant illuminance of the light, meaning that a more detailed calculation is unwarranted.

C1.7 Atmospheric optical depth has been widely studied, by measuring the attenuation of light as it passes vertically through the atmosphere from the edge of space to the surface of the planet (i.e. the attenuation of incoming light from the Sun or stars, or equivalently of out-going light from Earth as measured by satellites).

C1.8 The attenuation is made up of two[1] primary components. These are: (i) Rayleigh scattering by air molecules; and (ii) scattering and absorption by microscopic solid or liquid particles suspended in the atmosphere (aerosols). These are discussed in the next two sections.

C.2 Rayleigh scattering

C2.1 Scattering by particles whose size is much smaller than the wavelength of the light, such as air molecules in the atmosphere, is known as Rayleigh scattering. Rayleigh scattering has a characteristic wavelength dependence as roughly

$$\tau \propto \lambda^{-4}$$

where λ is the wavelength of the light (e.g. Penndorf 1957). Thus, bluer wavelengths are more strongly scattered (this is why the sky appears blue).

C2.2 The total optical depth for Rayleigh scattering vertically through the atmosphere has been well-established. It is given by (e.g. Hayes & Latham 1975; Buton et al. 2013):

$$\tau_{Rayleigh,atmos} \approx 0.14 \left(\frac{\lambda}{500\ \text{nm}}\right)^{-4} e^{(-h/h_0)}$$

where the numerical value corresponds to a wavelength λ of 500nm ($5\text{x}10^{-7}$m) which is appropriate for white light detected by the eye at low light levels (see Appendix B). In this equation, h is the height of the observer above sea-level, and h_0 is the scale-height of the atmosphere, set by the rate at which atmospheric pressure falls off with altitude.

C2.3 The atmospheric scale-height depends upon temperature, but for a temperature of 280K (around 7°C) it is typically $h_0 \approx 8$km.

C2.4 Optical depth is proportional to the number of scattering molecules, and therefore to the density of the air. Atmospheric density (ρ) largely follows pressure (apart from small effects of temperature variations with altitude) in falling off exponentially with altitude, $\rho \propto \exp(-h/h_0)$. Since

$$\int_0^\infty \exp\left(\frac{-h}{h_0}\right) = h_0$$

the optical depth of the atmosphere, viewed vertically to space from sea level, is equivalent to looking through a distance h_0 of atmosphere horizontally at sea-level.

C2.5 Given the large scale-height of the atmosphere, the density at an altitude of 390m above sea-level (the average hub altitude of the turbines in the Millmoor Rig Wind Farm) is still nearly 95% of that at sea-level. Thus, when looking horizontally at any altitude close to the Earth's surface, the optical depth due to Rayleigh scattering

[1] A third component of atmospheric attenuation, due to Ozone, is small ($\tau_{ozone} \approx 0.016$ along a vertical path from Earth to space) and in any case it can be ignored for the current analysis of horizontal attenuation near the Earth's surface, as the ozone is located at high altitude.

can be treated as a constant, depending only on the distance (D) between the light source and the observer,

$$\tau_{Rayleigh} \approx 0.14 \frac{D}{h_0} \left(\frac{\lambda}{500\ \text{nm}}\right)^{-4}$$

Thus the optical depth produced by air molecules in 1 km of atmosphere close to sea level is

$$\tau_{0,Rayleigh} \approx 0.018 \left(\frac{\lambda}{500\ \text{nm}}\right)^{-4}$$

C.3 Scattering by aerosols

C3.1 In addition to the normal molecular composition of air, air can contain additional components which restrict the passage of light. Common examples include dust and pollen, or man-made pollutants such as smoke or vehicle emissions. In maritime environments, sea salt is prevalent. Another common aerosol is liquid water droplets suspended in the air, as is the case for cloud or fog.

C3.2 It is common experience that under foggy conditions lights are visible for considerably shorter distances. For other aerosols, at typically much lower concentrations, the effect is less stark than for fog, but these still attenuate light, through scattering processes.

C3.3 For most aerosols the dominant scattering process is known as Mie scattering. The wavelength dependence of Mie scattering depends upon the nature of the scattering aerosol. Mie scattering is often expressed as a power law,

$$\tau \propto \lambda^{-\alpha}$$

where α is known as the Ångström exponent. Broadly speaking, the smaller the particle, the larger the value of α. For very small particles, Mie scattering tends towards Rayleigh scattering (α ~ 4). For large particles such as water droplets, which are very much larger than the wavelength of the light, the scattering become geometric, with no wavelength dependence (α = 0).

C3.4 Since for typical aerosols α is significantly below 4, the importance of Mie scattering compared to Rayleigh scattering increases for redder light. Mie scattering also differs from Rayleigh scattering in its directionality: Mie scattering tends to deflect light by relatively small angles.

C3.5 To model the attenuation due to aerosols, both the Ångström exponent and the density of aerosols are required. Like Rayleigh Scattering, the aerosol optical depth is generally measured along a vertical path between the surface of the Earth and space, either by ground-based instruments such as a LIDAR (Light Detection and Ranging) or from space, for example by MODIS (the Moderate Resolution Imaging Spectroradiometer) on NASA's Terra satellite. The total optical depth for aerosol scattering vertically through the atmosphere can be written as

$$\tau_{aerosol,atmos} \approx A_0 \left(\frac{\lambda}{500\ \text{nm}}\right)^{-\alpha} e^{(-h/h_{aerosol})}$$

where A_0 is the aerosol optical depth from sea-level to space at a wavelength of 500 nm, h is the height of the observer above sea-level, and $h_{aerosol}$ is the scale-height of aerosols in the atmosphere.

C3.6 The scale-height of aerosols is significantly smaller than that of the molecular content of the atmosphere. The precise value depends upon local conditions – both topology and weather. Hayes & Latham (1975) draw on data from many sets of measurements and argue for a typical scale-height of 1.5 km, while noting that it can vary by a factor of two from day to day. This value is widely adopted by many researchers. Matthias et al. (2004) analyse a significant dataset obtained from the European Aerosol Research Lidar Network in Aberystwyth and derive a typical scale height of 1.2km, again with significant variations. Other UK locations can be expected to be similar. In this report, a conservative value of $h_{aerosol}$ =1.5km is adopted.

C3.7 The aerosol optical depth is found to vary considerably with location on the Earth, being particularly high in polluted areas. In any given location, it also varies significantly with time.

C3.8 Estellés et al. (2002) measured A_0 over an 8-year period at a coastal location of the UK (Plymouth) and determined that it varied around a mean of 0.18 (median 0.19), with an (asymmetric) standard deviation of 0.08. The lowest observed value of the observed aerosol optical depth over this period was about 0.08. Matthias et al. (2004) found a median A_0 of 0.14 (after converting their data from 350 to 500nm), with a lower limit of around 0.06. Data available from the Aerosol Robotic Network (AERONET; see https://aeronet.gsfc.nasa.gov) found a median A_0 of 0.08 for Edinburgh.

C3.9 The proposed Millmoor Rig Wind Farm is in a relatively isolated location, away from large amounts of man-made pollutants, and away from the coast and thus sea-salt pollutants. Hence, the aerosol density might be expected to be relatively low. For the analysis in this report, the effect of a range of different A_0 values from 0.05 to 0.14 is therefore considered.

C3.10 Observed values of the Ångström exponent are typically in the range 0 to 1.5 (see discussion in Hayes & Latham 1975). Smirnov et al. (2002) argue that the exponent in maritime environments is α=0.3-0.7, while Estellés et al. (2012) found α =1.03±0.21 for their data taken at Plymouth. The Edinburgh AERONET data find a median α = 1.1. Larger values of α lead to lower values of attenuation for red lights, and so here a conservative value of α=1.2 is adopted. It should be stressed that the adoption of other reasonable values of α would not have a significant influence on the results (the effect of varying α is far smaller than the effect of the range of A_0 values considered above).

C3.11 As for Rayleigh scattering (C2.4), the aerosol optical depth as viewed vertically to space from sea level, is equivalent to looking through a distance of $h_{aerosol}$ of atmosphere horizontally at sea-level.

C3.12 Unlike Rayleigh scattering, the aerosol scale-height is low, and so the altitude above sea-level needs to be taken into account when considering the attenuation. For an altitude of 390m, and a scale-height of 1.5km, the aerosol density is around 77% of that at sea-level.

C3.13 Thus, following the arguments in C2.5, when looking horizontally at an altitude h, the optical depth due to aerosol scattering depends on the distance (D) between the light source and the observer as

$$\tau_{aerosol} = A_0 \frac{D}{h_0} \left(\frac{\lambda}{500\ \text{nm}}\right)^{-\alpha} \exp\left(\frac{-h}{h_0}\right)$$

Thus for typical conditions, using our best estimate parameters and assuming 390m altitude, we find an optical depth for 1 km distances of

$$\tau_{0,aerosol} = [0.025\ to\ 0.07] \left(\frac{\lambda}{500\ \text{nm}}\right)^{-1.2}$$

where the term in square brackets represents the range, due to the range of values to be adopted for A_0.

C.4 Resultant total attenuation under typical conditions

C4.1 Combining the optical depth for Rayleigh scattering with that from aerosols gives the total optical depth:

$$\tau = \tau_{Rayleigh} + \tau_{aerosol}$$

C4.2 At distance D, this is thus:

$$\tau \approx \left(0.018 \left(\frac{\lambda}{500\ \text{nm}}\right)^{-4} + [0.025\ to\ 0.07] \left(\frac{\lambda}{500\ \text{nm}}\right)^{-1.2}\right) \left(\frac{D}{1\text{km}}\right)$$

C4.3 From C1.1, the un-attenuated fraction of light is then f = exp(-τ). Figure C1 shows this attenuation both for white light (500nm) and for red light (633nm). The solid and dashed lines show, respectively, the fractions of remaining light given by the equation in C4.2, for the upper and lower ends of the range of A_0 values. The dotted lines show the contribution from Rayleigh scattering only.

C4.4 It can be seen that atmospheric attenuation has a significant effect, reducing light levels by factor of approximately 2 at 10km distance (depending on colour) in poorer aerosol conditions, with shorter (bluer) wavelengths of light being more strongly attenuated than longer (redder) wavelengths.

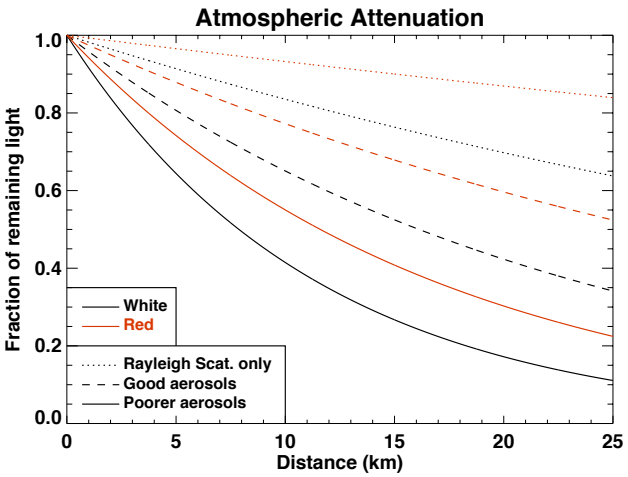

Figure C1: The attenuation of light as it passes horizontally through the atmosphere at an altitude of 390m. Results are shown for both white light (500nm) and red light (633nm). The dotted lines show the contribution from Rayleigh scattering by air molecules, in the absence of aerosols. The dashed and solid lines include aerosol attenuation under a range of realistic 'clear sky' conditions. It can be seen that atmospheric attenuation has a significant effect, particularly at larger distances. There is a dependence on colour, with redder light being less strongly attenuated.

C4.5 Combining this atmospheric attenuation with the geometric dilation of light discussed in Appendix A (Figure A1) then allows the total illuminance of a light as a function of distance to be derived, by multiplying the geometically-calculated illuminance by the un-attenuated fraction. This is shown for a 200 candela light in Figure C2.

C4.6 Figure C2 also compares the derived illuminance against other objects in the night sky, in particular the brightest star in the northern hemisphere, and typical bright stars in the constellation of Orion. It can be seen that at a distance of around 10km, the illuminance of a 200 candela red light is comparable to those of bright stars in the night sky.

C4.7 Figure C2 further shows that the choice of aerosol attenuation factor makes little qualitative difference to the perceived brightness of the lights, at least out to distances of 10km.

C.5 Reduction of illuminance of aviation lighting below the horizontal plane

C5.1 It is important to note that the calculations of Figure C2 assume the quoted candela value for the lights. Turbine lighting is highly directional, with the CAA candela requirements relating to the horizontal plane. At angles well below the horizontal plane, the luminous intensity of the aviation lighting is strongly suppressed, resulting in significantly lower illuminance. This will be relevant both for observers close to the turbines (who will typically be viewing them from below) and for population centres located at lower altitude.

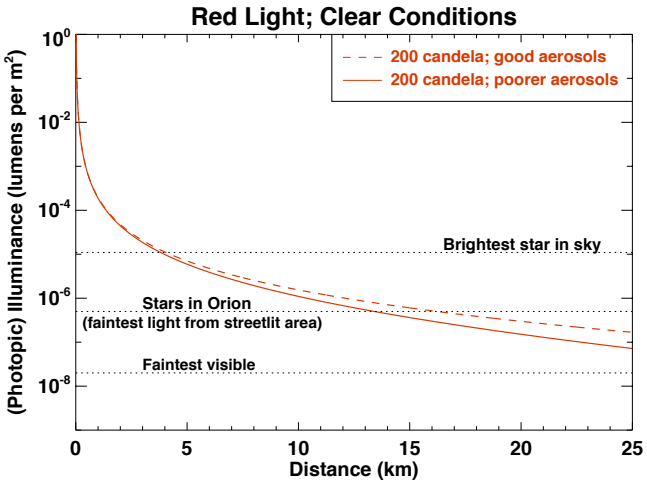

Figure C2: The illuminance of a single 200 candela red light (633nm) as a function of distance, viewed horizontally at an altitude of 390m. The results are shown considering the upper (solid line) and lower (dashed line) end of the realistic range of aerosol optical depth for typical clear conditions. For comparison, the illuminance provided by the brightest star in the northern sky is shown, along with those of typical bright stars such as those in the constellation of Orion. The latter also represent the approximate visual limit of the eye from street-lit areas (see Appendix B). Also indicated is the approximate visible limit to red light under perfect conditions (away from street lighting and other light pollution; new moon; dark-adapted eyes).

C5.2 To illustrate this effect, Figure 2 in the main report shows the vertical distribution of light using the technical specifications of a 2000 candela or 200 candela aviation LED currently available on the market, supplied by Contarnax Europe Ltd (CEL). This shows the strong suppression below the horizontal plane.

C5.3 If an aviation light is installed at a hub height of 100m then an observer at a distance of 2 km, at the same altitude as the base of the wind turbine, will be at an angle of nearly -3 degrees relative to the light's horizontal plane. For an aviation LED with CEL's specifications, this corresponds to a factor 10 suppression in candela rating, thus effectively converting a 200 candela light into a 20 candela light. At 4km the observer will be at an angle of -1.5 degrees, with about a factor of 3 suppression of light. Where the observer is on lower ground than the turbines, these suppression factors will be even greater.

C.6 Visibility

C6.1 An important factor for aviation lighting on wind turbines is the *visibility*. According to The Air Navigation Order regulations (Article 222) and the guidance in the Civil Aviation Authority Policy Statement of 1 June 2017 ('Lighting of onshore wind turbine generators in the United Kingdom with a maximum blade tip height at or in excess of 150m above ground level'), when the visibility is better than 5km the luminous intensity of the aviation warning lights may be reduced from 2000 to 200 candela.

C6.2 Visibility relates to the attenuation of light. It is defined by the World Meteorological Organisation as the distance at which the intrinsic brightness of a light is reduced to 5% of its initial value due to light attenuation (i.e. excluding the $1/D^2$ geometric dilution discussed in Appendix A). It is usually defined at 550nm.

C6.3 Visibility and optical depth are directly related. At the 5% visibility threshold,

$$\exp(-\tau) = 0.05.$$

This corresponds to τ=3.0.

C6.4 As discussed in C2.5, the contribution of Rayleigh scattering at 550nm to the optical depth at a distance of 5km is only $\tau_{Rayleigh}$ = 0.06, and thus aerosol scattering completely dominates the opacity in poor visibility conditions.

C6.5 In such poor visibility conditions, the opacity is generally associated with larger particles such as liquid water droplets (cloud or fog), and hence a lower value of the Ångström exponent is appropriate. Here a value of α=0.6 is assumed, but again the results are not critically dependent upon the choice. For α=0.6, the opacity at 633nm at the visibility threshold is τ = 2.6 at 5km, corresponding to an optical depth per km of τ_0 = 0.52.

C6.6 In such poor visibility conditions, a 2000 candela light is required. Figure C3 shows the illuminance of such a light as a function of distance, accounting for atmospheric attenuation at the threshold value. This is a worst-case scenario for 2000 candela lighting: in better conditions the luminous intensity of the lighting can be reduced, while in poorer conditions the atmospheric attenuation effects will be increased.

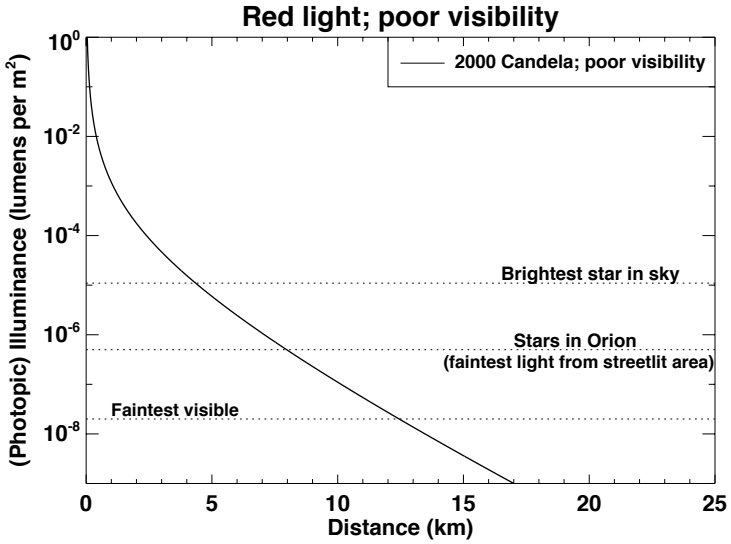

Figure C3: The illuminance of a 2000 candela light as a function of distance, as observed when the visibility conditions for the wind farm are at the threshold limit for requirement of such lights (visibility = 5%). This is compared against the illuminance provided by bright stars in the night sky.

C6.7 Figure C3 shows that, beyond about 5km from the wind turbine, the illuminance of this light drops below that of the brightest stars in the night sky.

C6.8 Zhang et al. (2020) give an overview of different techniques for measuring visibility. As locally-derived data are not available for the distribution of visibilities on the proposed Millmoor Rig Wind Farm site, an estimate can be made using the public data on visibility measurements available in other locations around Scotland.

C6.9 A dataset is available from the Leuchars air base in Fife, that stretches back for 60 years (Singh et al. 2017). Leuchars is subject to broadly the same weather conditions and prevailing wind direction as the Scottish Borders area, and therefore can be expected to provide similar results. The visibility distribution for Leuchars for the past two decades is shown in the upper panel of Figure C4. Based on these data, the visibility at Leuchars drops below 5km for between 3 and 4% of the time.

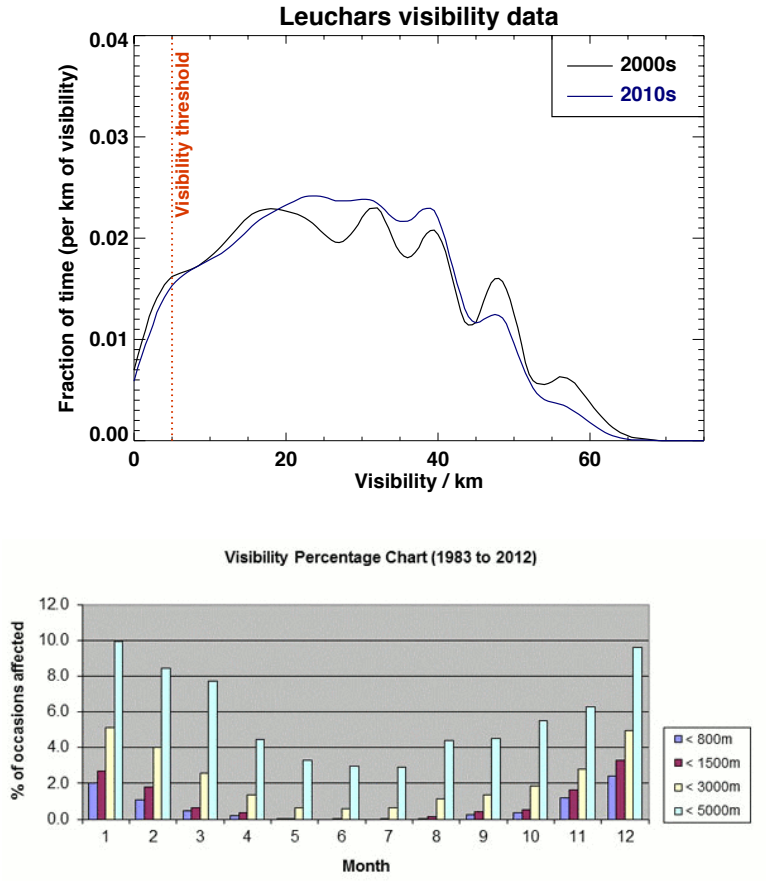

Figure C4: Top: the distribution of visibilities measured at the Leuchars air base over the past two decades (data from Singh et al. 2017). Bottom: the published visibility chart for Carlisle airport [Credit: Met Office].

C6.10 Climate statistics are also published by the Met Office for various UK airports (see references). The Millmoor Rig Wind Farm lies towards the centre of a triangle formed by Carlisle airport (about 48km from the windfarm), Edinburgh airport (82km away) and Newcastle airport (65km away). The Met Office data for the closest of these, Carlisle airport, are shown in Figure C4 and similarly show that visibility drops below 5km for between 5 and 6% of the time, averaged across the year (being lowest in summer and highest in winter).

C6.11 The data from Edinburgh airport indicates that visibility there drops below 5km for just over 6% of the time on average, while Newcastle airport has a higher fraction of time affected by poor visibility (about 11% of the time). Data from other airports in southern Scotland indicate poor visibility for fractions of between 4% and 7% of the time. The slightly higher values for Edinburgh and particularly Newcastle airports, compared to Leuchars and Carlisle airport, may well be associated with the proximity to the large population centres, where man-made pollutants will be higher.

C6.12 Edinburgh, Newcastle and Carlisle airports, and Leuchars, are all located close to sea level. Although aerosol densities decrease with increasing altitude, higher altitude sites like the Millmoor Rig Wind Farm are more likely to be affected by cloud or mist. For this reason, a conservative estimate is that the Millmoor Rig Wind Farm may be affected by poor visibility for up to 10% of the time.

C.7 Total ambient light level of the wind farm

C7.1 The proposed lighting scheme for the Millmoor Rig Wind Farm includes 5 turbines with visible lighting. In Figure C5, the total illuminance provided by the sum total of all of these turbine hub lights is assessed as a function of distance, and compared to natural ambient light levels. The analysis assumes that all turbines are located at the same distance from the observer. Results are shown for distances of 3km to 25km, as at smaller distances the overall extent of the wind farm means that the assumption of equal distance to all turbines is poor.

C7.2 The analysis also assumes that the maximum luminous intensity of the turbines is seen which, as discussed above, will over-estimate the effect below the horizontal plane due to the directionality of the light.

C7.3 The results indicate that, even in the worst-case scenario, the contribution of the whole wind farm development is comparable to, or below, the ambient background levels produced by starlight in a moonless sky, at all distances beyond 3 km.

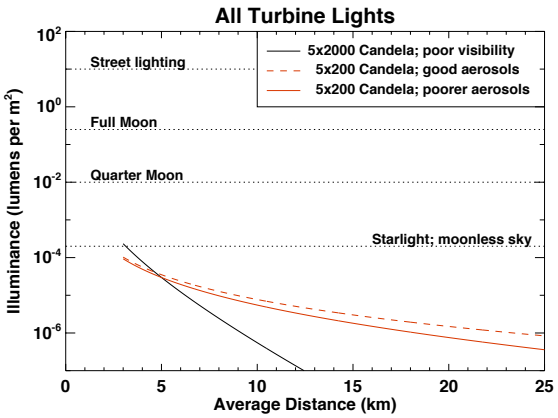

Figure C5: The total illuminance provided by all turbine hub lights as a function of distance, compared to natural and man-made ambient light backgrounds. The red solid and dashed lines show respectively the upper and lower end of the range of aerosol optical depths considered for 'clear' conditions. The black line shows poor visibility conditions when 2000 candela lights are mandated. In all cases, the assumption is made that all turbines are visible, and all are located at the same distance (this will not be valid for small distances). As is evident, for all distances beyond 3 km the total ambient light level produced by the wind farm is below that of the starlit moonless sky.

Appendix D: Turbine and Viewpoint locations

D1.1 Table D1 provides details of the turbine locations, and indicates which turbines will carry visible lighting, according to the lighting scheme approved by the CAA.

D1.2 Table D2 provides details of the 21 representative viewpoints considered in the LVIA analysis, and which form the basis for the calculations in the current report.

Turbine No.	OS Grid Reference	Visible lighting?
1	363467, 605540	Yes
2	363225, 606000	
3	363500, 606716	Yes
4	362806, 606357	
5	362152, 606085	
6	362073, 605489	
7	362314, 607067	
8	361771, 607162	Yes
9	360583, 606704	Yes
10	360977, 606405	
11	361140, 605737	
12	361395, 605389	Yes
13	361667, 606243	

Table D1: Locations of the 13 turbines in the proposed Millmoor Rig Wind Farm, and indication of which will carry visible aviation lighting.

Viewpoint No.	Location	OS Grid Reference
1	A6088, Chesters	362395, 610476
2	A6088, Southdean	363250, 609112
3	Fort north-east of Southdean	363496, 609388
4	A6088, Western approach to Chesters	361634, 610634
5	Bonchester Hill	359471, 611790
6	B6357 Vantage Point	359170, 603557
7	Footpath at Knox Knowe	365468, 602816
8	A6088, north-west of Carter Bar	367569, 607371
9	Carter Bar (eastern vantage point)	369798, 606857
10	Pike Fell	353489, 606367
11	Footpath and Minor Local Road, Chesters Brae	363279, 610785
12	Rubers Law	358048, 615547
13	A6088 Approach to Bonchester Bridge	355994, 612670
14	Wolfelee Hill	359717, 608474
15	Pennine Way, Black Halls	378828, 610659
16	Five Stanes	375263, 616863
17	A7 Approach to Hawick	351069, 616778
18	Borders Abbey Way, Black Law	361964, 618201
19	Wheel Causeway	361280, 601935
20	A68, north of hairpin past Carter Bar	368973, 608692
21	Rowan Road, Jedburgh	366084, 620422

Table D2: Details of the 21 LVIA viewpoints considered in this report. Viewpoint numbers correspond to those in Table 2.

References

Air Navigation Order 222;
https://www.caa.co.uk/general-aviation/the-ga-unit/air-navigation-order-2016/

Blackwell H.R., 1946, Journal of the Optical Society of America, Vol. 36, Issue 11, p624

Blackwell O.M. & Blackwell H.R., 1971, Journal Illuminating Engineering Society, 1, 3.

Buton C. et al., 2013, Astronomy & Astrophysics, 549, A8.

CAA Policy Statement 1st June 2027 on 'Lighting of onshore wind turbine generators'
https://www.caa.co.uk/publication/download/16178

CAP-764; https://www.caa.co.uk/publication/download/14561

CEL Technical Specifications for 2000 candela ANO light

Cinzano P., Falchi F., Elvidge C.D., 2001, Monthly Notices of Royal Astronomical Society, 323, 34.

Crawford B.H., 1949, Proceedings of the Physical Society, B62, 321.

Crumey A., 2014, Monthly Notices of Royal Astronomical Society, 442, 2600.

Estellés V., Smyth T., Campanelli M., 2012, Atmos. Environment, 61, 180.

Falchi F. et al., 2016, Science Advances, 2, e1600377.

Hayes D.S. & Latham D.W., 1975, Astrophysical Journal, 197, 593.

Judd D.B., 1951, `Report of U.S. Secretariat Committee on Colorimetry and Artificial Daylight.', Proceedings of the Twelfth Session of the CIE, Stockholm, Vol.1, p11.

Knoll H.A, Tousey R., Hulburt E.O., 1946, Journal of the Optical Society of America, Vol. 36, Issue. 8, p480.

Matthias et al 2004, Journal Geophysical Research, 109, D18201.

Met Office airport climate statistics;
https://www.metoffice.gov.uk/services/transport/aviation/regulated/airfield-climate-stats

Penndorf R., 1957, J. Opt. Soc. Amer.,47, 176–182.

Singh A., 2017, Atmos. Chem. Phys., 17, 2085

Smirnov et al 2002, Journal of Atmospheric Science, 59, 501.

Vos J.J., 1978, Color Research & Application, 3, 125.

Wald G., 1945, Science, 101, 653.

Zhang S., 2020, Earth Science Review, 200, 102986